International Journal of Biometeorology (2023) 67:847–856
https://doi.org/10.1007/s00484-023-02459-7

ORIGINAL PAPER

Influence of monsoon anomalies on intra-annual density fluctuations of Chinese pine in the Loess Plateau

Shuangjuan Wang[1] · Yang Deng[1] · Linlin Gao[1] · Yuhang Zhang[1] · Xingying Shi[1] · Xiaohua Gou[1]

Received: 20 October 2022 / Revised: 8 February 2023 / Accepted: 17 March 2023 / Published online: 28 March 2023

Abstract

In the past few decades, the East Asian summer monsoon (EASM) has experienced an unprecedented weakening, exacerbating drought in northern China, especially in the monsoon margin area. Improving our understanding of monsoon variability will benefit agricultural production, ecological construction, and disaster management. Tree-ring is widely used as proxy data for extending the monsoon history. However, in the East Asian monsoon margin, the tree-ring width were mostly formed before the rainy season, thus may have limited ability to indicate the monsoon variability. Intra-annual density fluctuations (IADFs) can provide higher resolution information on tree growth as well as evidence of short-term climate events. Here, we used Chinese pine (*Pinus tabuliformis* Carr.) samples from the eastern edge of the Chinese Loess Plateau (CLP), where the climate is deeply affected by monsoon, to investigate the response of tree growth and IADFs frequency to climate variation. We show that tree-ring width and IADFs record significantly different climatic signals. The former was mainly affected by moisture conditions at the end of the previous growing season and the current spring. While the latter was common in years when severe droughts occurred in June and July, especially in June. This period coincides with the onset of the EASM, so we further analyzed the relationship between IADFs frequency and the rainy season. Both correlation analysis and the GAM model suggest that the frequent occurrence of IADFs may be related to the late start of the monsoon rainy season, meaning that we have found a new indicator in tree-ring records that can capture monsoon anomalies. Our results provide further insight into drought variation in the eastern CLP, which also implicates the Asian summer monsoon dynamic.

Keywords Tree-ring · IADFs · Climatic response · Rainy season · Cambial activity

Introduction

As one of the most active components of the Northern Hemisphere summer climate system, the variability of the East Asian summer monsoon (EASM) deeply affects the lives and well-being of more than one billion people. Since the 1970s, the EASM has shown an obvious weakening trend (Wang 2001; Yu et al. 2004), resulting in later and less precipitation in northern China (Ding et al. 2008; Li 2013). Under the combined effect of rapid warming in the past decades, the drought in northern China, especially in the margin of EASM, has been further aggravated (Dai et al. 2003; Ma and Dan 2005; Ma and Fu 2006), which has greatly affected agricultural production and ecological construction (Qin et al. 2014; Bo et al. 2015; Zhang et al. 2016; Zhao et al. 2019). Improved knowledge of monsoon variability would benefit risk management in the agricultural, ecological, and hydrological. However, instrumental climate data are generally limited in length, which hamper our full understanding of monsoon dynamics. Therefore, exploring possible proxy of monsoon variability is critical.

As a high-resolution proxy data, tree-ring has unique advantages in paleoclimate research. However, tree radial growth is driven not only by current year's climatic conditions, but also by prior years (Kagawa et al. 2006), thus insufficient to reflect short-term climate events. Besides tree-ring width, many xylem anatomical features at the cellular scale are able to record intra-annual climate variation (Eilmann et al. 2009; Fonti et al. 2010; Cuny et al. 2014; Zhu et al. 2017), such as common intra-annual density fluctuations (IADFs).

✉ Yang Deng
dengy@lzu.edu.cn

✉ Linlin Gao
gaoll@lzu.edu.cn

[1] MOE Key Laboratory of Western China's Environmental Systems, College of Earth Environmental Sciences, Lanzhou University, Lanzhou 730000, China

Environmental stress during the growing season makes trees enter the dormant period prematurely, thus resulting in the formation of latewood-like cells in earlywood, and when this stressor disappears or is alleviated, the trees resume normal physiological activity with the appearance of earlywood-like cells, which is reflected in IADFs and commonly called false ring (De Micco et al. 2016). IADFs is an abrupt changes in xylem anatomy caused by trees' adjustment strategy to short-term climate change (Campelo et al. 2007; De Micco et al. 2016), and thus can provide climate-ecological information at seasonal scales as well as evidence of extreme climate events (Panayotov et al. 2013; Battipaglia et al. 2016). The Mediterranean climate zone is currently the main focus of IADFs research, which provides useful information on the effects of summer drought on intra-annual tree growth (Zalloni et al. 2019; Piermattei et al. 2020). However, there are fewer IADFs related studies in East Asia to date, such as northern China, because the region has fewer summer droughts and shorter tree growing seasons than the Mediterranean.

The Chinese Loess Plateau (CLP) lies in the transition zone between a semi-humid monsoon climate and an inland arid and semi-arid climate, where seasonal precipitation is highly uneven and variable due to the monsoon's advance and retreat, and seasonal drought is common due to asynchronous summer rain and heat. Moreover, this characteristic is becoming increasingly prominent in the context of global warming and monsoon decline. Accordingly, many tree-ring-related studies (Song and Liu 2011; Li et al. 2022) have been conducted in the CLP in recent years. However, regional tree-ring records mostly reflect the drought variability in spring and summer before monsoon onset, thus providing limited information on monsoon dynamics. The end of the dry season in this area is clearly marked by the onset of the rainy season, so the short-term drought signal contained in IADFs may also imply a monsoon anomaly. Related studies in other monsoonal regions have pointed out this possibility (Singh et al. 2016; Babst et al. 2016). Chinese pine (*Pinus tabuliformis* Carr.), a main native species of the CLP, is prone to IADFs based on xylem anatomy (Gao et al. 2021a). However, no IADFs chronology for Chinese pine or CLP has been reported so far.

Since IADFs and tree-ring width are driven by climatic conditions at different time scales, we hypothesize that they record different climatic signals. Besides, late monsoon may result in drought during growing season and thus increased the possible of IADFs occurrence; therefore, IADFs frequency may provide information on monsoon dynamics. In this study, we established ring width and IADFs frequency chronologies of Chinese Pine in the east edge of the CLP, clarified the climate signal recorded by IADFs and tree-ring width, and explored the possible influence of the EASM on IADFs frequency.

Materials and methods

Study area

This study was carried out in a semi-humid forest in the eastern edge of the CLP (Fig. 1(a)). According to the observation records of the Zuoquan Meteorological Station (37° 4′ 48″ N, 113° 21′ E, 1091.4 m a.s.l., 1959–2014 CE), the closest meteorological station to the sampling site (32 km), the average annual total precipitation is 233 mm, and the seasonal distribution is uneven (Fig. 1(c)). The concentrated precipitation brought by the monsoon from June to September accounts for about 72% of the whole year. The annual average temperature is 7.8 °C, with the coldest January averaging − 7.9 °C and the hottest July averaging 21.4 °C. Over the last 56 years, the regional climate has experienced significant warming (Fig. 1(d)), while the trend for precipitation is insignificant (Fig. 1(e)).

Tree-ring data

In the summer of 2019, a pure Chinese pine forest (37° 01′ 35″ N, 113° 41′ 55″ E, 1230–1330 m a.s.l., Fig. 1(b)) was selected from Zuoquan County, Shanxi Province. One or two cores per tree in different directions at the DBH (1.2–1.5 m) were sampled from healthy, mature, undisturbed trees with increment borer. A total of 49 cores from 26 trees were collected, and then the samples were brought back to the laboratory. According to the international standards (Stokes and Smiley 1968), all cores were fixed on grooved wooden strips to dry naturally, and polished with 200, 400, and 600 grit sandpaper accordingly, until the xylem cell structure was clearly visible under the microscope. Visual dating was carried out under a binocular microscope, and the tree-ring (TRW), earlywood (EW), and latewood width (LW) were measured using the Velmex Measuring System with an accuracy of 0.001 mm. The cross-dating quality was checked with TSAP-Win and COFECHA programs (Holmes 1983). The non-climatic signals caused by tree age and stand dynamics were removed by fitting linear and negative exponential curves (with a few poorly fitted selected spline functions) using the ARSTAN program (Cook 1985). The de-trended TRW, EW, and LW indices were averaged using the biweight robust means to create three standardized (STD) chronologies. In addition, the strong linear correlation between EW and LW was removed with the method proposed by Meko and Baisan (2001), to obtain an adjusted latewood width series (LW_{adj}).

Intra-annual density fluctuations

We identified IADFs in 43 cores (excluding six cores that did not reach the pith) and divided them into two groups

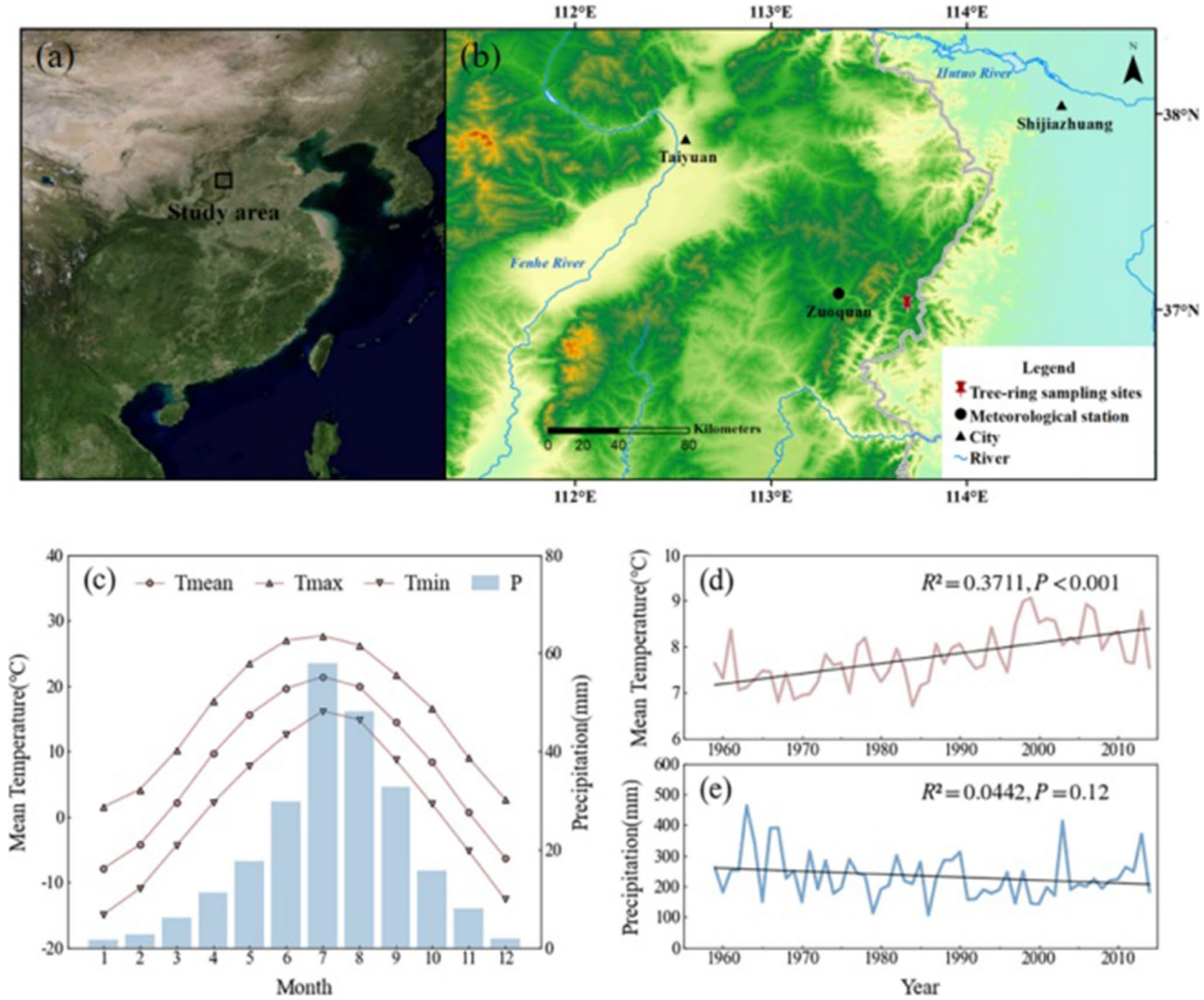

Fig. 1 Location of the study area (**a**), sampling site and meteorological station (**b**). Intra-annual distribution of monthly mean, maximum, minimum temperature and precipitation (**c**), and inter-annual trends of annual mean temperature (**d**) and annual precipitation (**e**) at Zuoquan meteorological station from 1959 to 2014

(E-IADFs and L-IADFs), according to the relative position of IADFs within the tree rings. E-IADFs are characterized by a band of latewood-like cells appearing in the earlywood, while L-IADFs are characterized by a band of earlywood-like cells appearing in the latewood (Fig. S1).

A large number of studies show that IADFs appear more frequently in younger trees, and this age trend may interfere with our understanding of the climate signals recorded in IADFs chronology (Novak et al. 2013; De Micco et al. 2016). In order to eliminate the influence of cambium age on IADFs frequency, we used binomial logistic model to fit the age trends of 43 series of statistical IADFs, with the independent variable being cambium age and the dependent variable being the presence or absence of IADFs (1 for presence and 0 for absence) (Zalloni et al. 2016). The residuals of each logistic model were then averaged over the corresponding years to finally obtain an IADFs frequency index chronology without age trend. It should be noted that the cambium age at the time of the occurrence of IADFs ranged from 2 to 201 years.

Climate data

Monthly average maximum temperature, average temperature, and precipitation data from the Zuoquan station, as well as the standardized precipitation-evapotranspiration index (SPEI, Vicente-Serrano et al. 2010) at a 1-month scale calculated from this station data, were used to determine the effects of climatic factors on tree growth. SPEI represents the water surplus and deficit by the monthly difference

between precipitation and potential evapotranspiration, and its value can be used to assess the dry and wet states of the regional climate (Vicente-Serrano et al. 2010). SPEI was calculated using the R package "SPEI" based on the Thornthwaite equation (Beguería et al. 2017).

To explore the possible association between the IADFs frequency and the monsoon rainy season, we calculated the start date of single-station rainy season by referring to the method proposed by Li and Guo (2015). The daily precipitation data used in the calculation are also from the Zuoquan station. The calculation method is detailed in supplementary materials.

Statistical analysis

The Pearson correlation coefficients between tree-ring width chronologies and climate variables were calculated to investigate the climate signals recorded by tree growth. As the residuals of the logistic regression model do not obey a normal distribution, the Spearman correlation coefficients between the IADFs frequency index chronology and climate variables and the start date of the rainy season were computed. Climate variables include monthly average maximum temperature, average temperature, precipitation, and SPEI. The monthly climate data from previous May to current September and from current March to September were used for the ring width chronologies and the IADFs chronology, respectively.

We defined the years with IADFs frequency index greater than its third quartile (1.075) from 1959 to 2014 as "high IADFs" (HI) years. Superposed epoch analysis (SEA) was used to examine whether the monthly average maximum temperature, average temperature, precipitation, and SPEI from March to September in 14 HI years were statistically different from other years chosen randomly. One thousand Monte Carlo simulations were performed to test the statistical significance of monthly climate anomalies in HI years. The SEA was computed using the R package "sea_dbl" (Rao et al. 2019).

The generalized additive model (GAM) was used to analyze the relationship between the start date of the rainy season and IADFs frequency index. The GAM model, as a non-parametric extension of the traditional generalized linear model, can effectively deal with the complex nonlinear and non-monotonic relationship between explanatory variables and response variables, and does not need to make too many assumptions about the relationship between variables. The GAM was fitted using the R package "mgcv" (Wood 2006).

Results

Tree-ring width and IADFs chronologies

The four tree-ring width chronologies are shown in Fig. 2. The trends and extreme values of TRW, EW, and LW are very similar, but LW differs in some years (e.g., 1877, 1887, 1935, 1976). In the period from 1959 to 2014, for which meteorological data are available, the maximum value of the chronologies occurred in 1964 and the minimum value in 2009. In 1964, meteorological records showed much higher precipitation during the growing season, resulting in a wide ring. In 2009, a severe drought occurred in the previous autumn and winter and the current growing season, generating a narrow ring. The descriptive statistics in Table 1 indicate that all three chronologies have high sensitivity, with mean sensitivity (MS) ranging from 0.56 to 0.68. They also have strong and consistent common signals, with EPS from 0.94 to 0.96 and RBAR from 0.44 to 0.55.

A total of 5299 tree rings were involved in IADFs statistics, and 1068 rings had IADFs (20%), of which 952 E-IADFs, 28 L-IADFs, and 88 E- and L-IADFs co-occurring

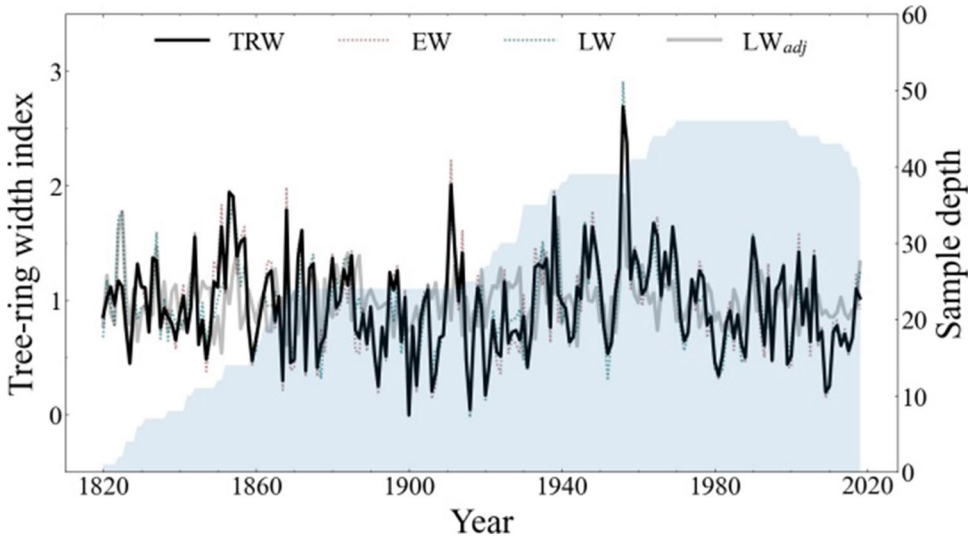

Fig. 2 Standard chronologies of tree ring (TRW), earlywod (EW), latewood (LW) and adjusted latewood width (LW_{adj}) of Chinese pine from 1820 to 2018. The blue field represents the sample depth for each calendar year

Table 1 Descriptive statistics of the tree-ring standard chronology

Basic statistics	TRW	EW	LW
RBAR	0.553	0.559	0.358
EPS	0.959	0.96	0.914
SNR	23.51	24.065	10.594
MS	0.421	0.49	0.376
AC1	0.384	0.286	0.494

RBAR correlation of mean intersections, *EPS* expressed population signal, *SNR* signal-to-noise ratio, *MS* mean sensitivity, *AC1* first-order autocorrelation

in a single ring. As there were too few L-IADFs, only E-IADFs (including E-IADFs occurring alone and co-occurring with L-IADFs, 1040 in total) were selected for subsequent analysis. Figure 3 shows the IADFs frequency index chronology obtained by calculating the mean of the logistic model residuals to remove the age trend. We observed that the IADFs frequency index was not significantly related to TRW, EW, and LW, but significantly positively correlated with LW_{adj} ($r = 0.36$, $p < 0.001$).

Climate responses of ring width and IADFs chronologies

The climate signals reflected by TRW, EW, and LW are quite similar, with only slight differences in the correlation coefficients (Fig. 4). The correlations with temperature are generally negative, with significant correlations observed between average maximum temperature in September of the previous year and April and May of the current year (Fig. 4(a)), while correlations with average temperature are all insignificant (Fig. 4(b)). The correlations with precipitation are significantly positive in July and September of the previous year and in April of the current year (Fig. 4(c)). LW_{adj} shows a significantly positive correlation with average temperature in June of the current year and precipitation in January and September of the current year (Fig. 4(b) and (c)).

A negative correlation with temperature and a positive correlation with precipitation, indicating a typical drought response pattern, so we further analyzed the relationship between chronologies and SPEI. The correlations between TRW, EW, LW, and SPEI are mostly significantly positive in July and September of the previous year and April of the current year, while LW_{adj} and SPEI is only significantly positive in September of the current year (Fig. 4(d)). This means that the growth of Chinese pine is mainly influenced by the moisture conditions at the end of the growing season of the previous year and in April of the current year.

The Spearman correlation analysis shows that the IADFs frequency index is mainly positively correlated with average maximum temperature in April, June, and July, average temperature in June, and negatively correlated with precipitation and SPEI in June (Fig. 5). SEA shows not exactly the same results. HI years are associated with high temperatures in June and July and low precipitation and SPEI in June (Fig. S2). This suggests that IADFs tend to occur in years with climate anomalies in June and July, especially in June, when high temperatures, low precipitation, and abnormal droughts are observed.

Relationship between IADFs frequency and rainy season

The precipitation of the CLP is highly concentrated from June to August, which was deeply affected by the EASM. The regional rainy season usually starts from late June to early July, and delayed onset may lead to early summer droughts, which occur at the same time as the abnormal drought in the high frequency years of IADFs. Therefore, there may be a possible linkage between monsoon activity and IADFs.

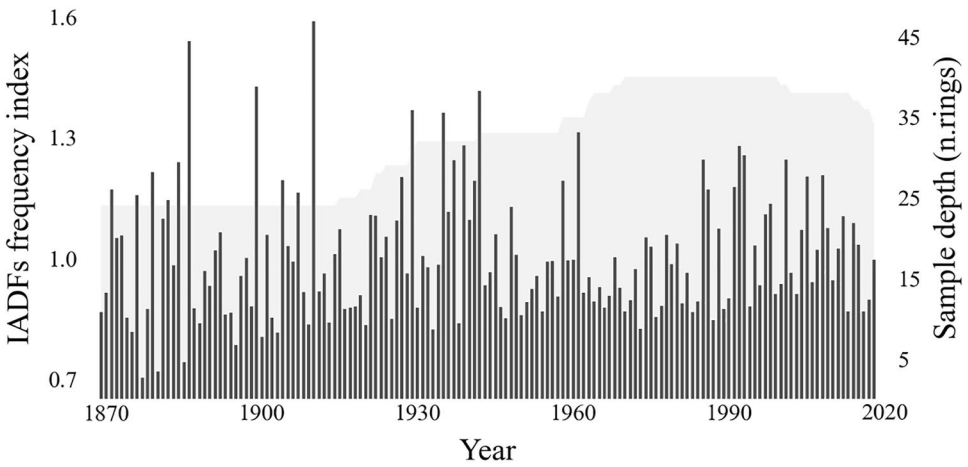

Fig. 3 IADFs frequency index chronology from 1869 to 2018. The dark gray bars and light gray fields represent the IADFs frequency index and sample depth at each calendar year, respectively

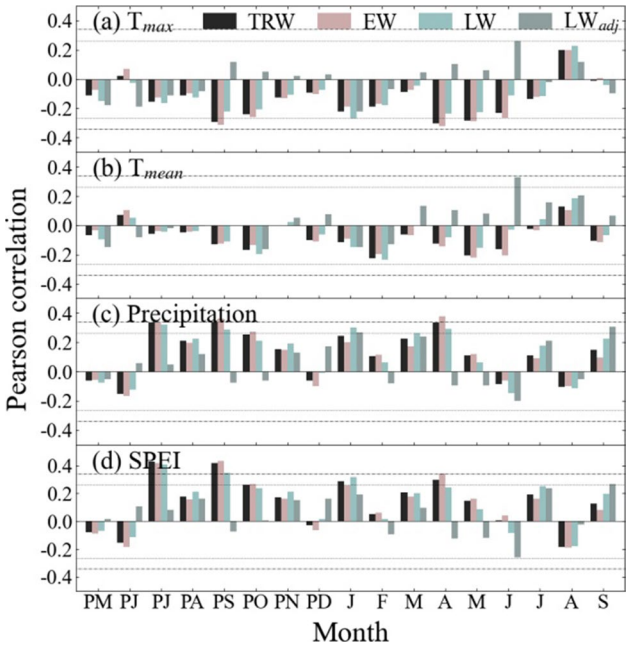

Fig. 4 Pearson correlation coefficients between Standard chronologies of tree ring (TRW), earlywod (EW), latewood (LW), adjusted latewood width (LW_{adj}) and monthly average maximum temperature (T_{max}) (**a**), average temperature (T_{mean}) (**b**), precipitation (**c**), and SPEI (**d**) from previous May (PM) to current September (*S*). Correlations were calculated for the period from 1960 to 2014. Dashed horizontal lines show the 0.05 and 0.01 significance levels

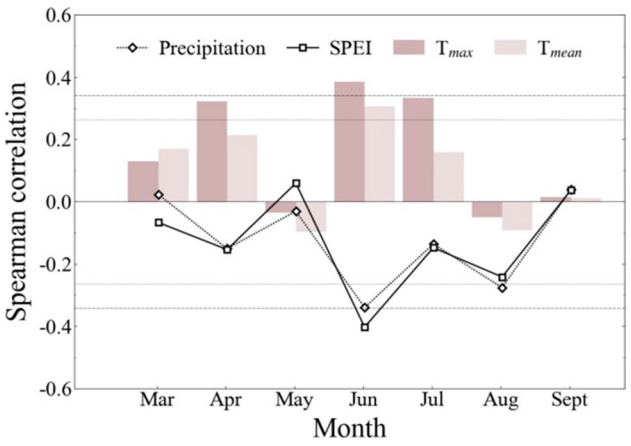

Fig. 5 Spearman's correlation coefficients between IADFs frequency index and monthly average maximum temperature (T_{max}), average temperature (T_{mean}), precipitation, and SPEI from March to September. Correlations were calculated for the period from 1959 to 2014. Dashed horizontal lines show the 0.05 and 0.01 significance levels

We calculated the rainy season onset time based on daily precipitation from the Zuoquan station, and examined its relationship with the IADFs frequency. The results demonstrate that there is a strong positive correlation between them (Fig. 6, $r = 0.44$, $p < 0.001$), and this correlation is significant in two time periods: 1959–1986 ($r = 0.4$, $p < 0.05$) and 1987–2014 ($r = 0.43$, $p < 0.05$). GAM further evaluated the impact of the start date of the rainy season on the IADFs frequency. In the model, the total deviation explained by the prediction factors is 22.5%, and the adjusted R^2 is 0.21. Therefore, the onset time can be considered a significant factor affecting the IADFs frequency. Moreover, according to the estimated degree of freedom of the smoothed variable (EDF = 1), the two are linearly dependent, that is, the later the rainy season starts, the higher the IADFs frequency appears (Fig. 7).

Based on the above relationship, we speculate that the EASM variability before instrumental data may be greater. For example, the IADFs values in 1886, 1899, and 1910 were very high, so the monsoon may be abnormally late. The values in 1877, 1881, and 1885 were very low, the monsoon may have arrived much earlier. In addition, since the late 1970s, the years with a high frequency of IADFs have increased (such as 1985, 1986, 1991, 1992, 1993, 2005, 2008), which corresponds to the weakening trend of EASM.

Discuss

Ring width and IADFs record different climate signals

In this study, tree growth was mainly influenced by the moisture conditions at the end of the previous growing season and in the spring of the current year (Fig. 4), in line with many tree-ring studies in the CLP (Fang et al. 2012; Chen et al. 2014; Li et al. 2022). In autumn, the division activity of tree cambium is close to the end, but photosynthesis is still vigorous if temperature and soil moisture are appropriate, the synthesis and storage of non-structural carbohydrates will have a "lagging" effect on earlywood growth in the following spring (Rolland 1993; Larsen and MacDonald 1995). Wood anatomy and experimental studies have shown that soil water availability is a key driver of xylogenesis, affecting all stages of tracheid development, with cell production and expansion stages considered to be the most sensitive (Hsiao 1973; Peters et al. 2021). The cambium of Chinese pine became active in late spring, the number of cambium cells peaked between May and June, and cell enlargement peaked in June (Gao et al. 2021b). However, precipitation in the CLP is highly concentrated in summer, and low soil moisture before the rainy season may shorten the time of cambium activity (De Luis et al. 2011), reduced cell production (Swidrak et al. 2011), and limit cell expansion (Abe and Nakai 1999; Gruber et al. 2010), eventually leading to less radial growth and abnormal anatomical characteristics (Eilmann et al. 2011; Martin-Benito et al. 2013). For example, Gao et al. (2021a)

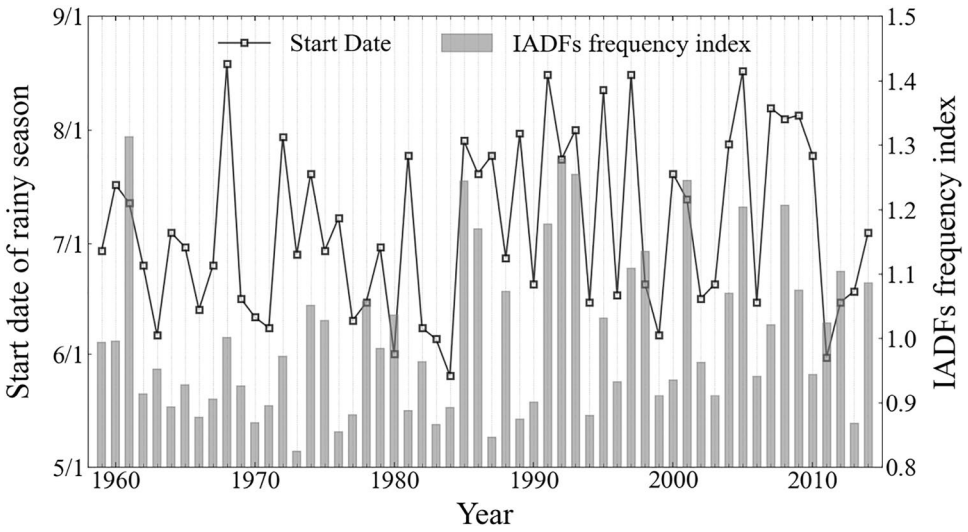

Fig. 6 Interannual variation of the IADFs frequency index and the start date of the rainy season from 1959 to 2014. The Spearman correlation coefficient of the two sequences is 0.44 ($p < 0.001$). The unit of the "Start date of rainy season" is a day. The *y*-axis labels 5/1, 6/1, etc. represent May 1, June 1, and so on

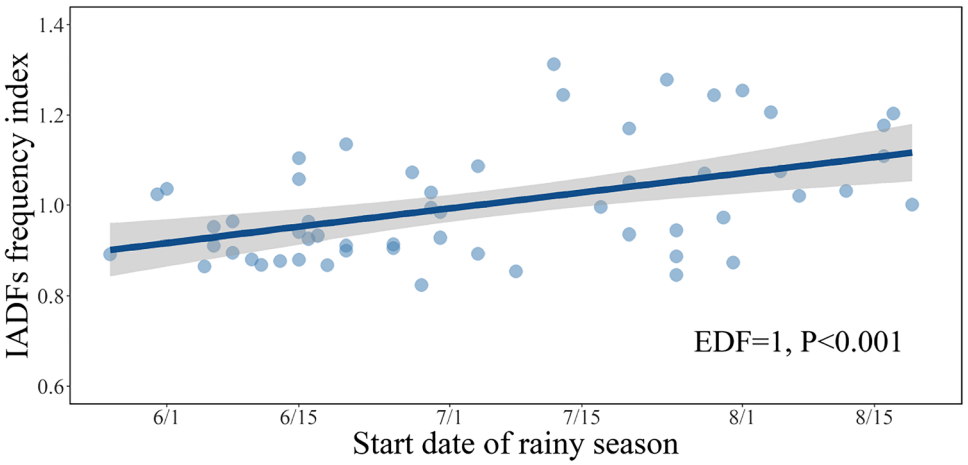

Fig. 7 The generalized additive model (GAM) was performed with the IADFs frequency index as the response variable and the start time of the rainy season as the explanatory variable. EDF refers to estimated degree of freedom of the smoothed variable in the single-factor model. The smoothed best-fit line with 95% confidence interval

monitored the cambium activity and wood formation of Chinese pine in Helan Mountain, northwest of the CLP, and found that the drought in June restricted the cell production of cambium, resulting in only 36% xylem cells formed at that time. And led to unfavorable conditions for cell expansion, the lumen contracted to a narrow latewood cell size, forming E-IADFs. In the rings without IADFs, 68% of the cells were produced in June, and these cells completed cell expansion, showing a faster xylem formation process, which may be due to more late spring and summer precipitation.

Wood formation monitoring demonstrates that E-IADFs are closely associated with climate stress during the growing season on the microscopic scale, while the frequent and stable occurrence of IADFs in the tree rings may indicate common climate signals on the macroscopic scale (Vieira et al. 2017; Arzac et al. 2018; Pacheco et al. 2020). The IADFs in this study were triggered by climate anomalies in June and July, especially in June when the temperature was higher and the precipitation was less (Fig. 5, Fig. S2). In addition, the average maximum temperature in April also showed a significant impact. High temperature in the early growing season may advance cambium activity and increase transpiration, exposing trees to longer and stronger droughts (Begum et al. 2013). Under persistent high temperatures and severe water deficits in June and July due to delayed rainy season, soil moisture and xylem water potential decreased further (Nonami and Boyer 1990). When the water pressure inside the cell exceeds that outside, the cell expands (Lockhart 1965). Under low turgor pressure, trees form latewood-like cells with small diameter and thick cell wall to minimize the risk of xylem embolism by drought (Abe and Nakai 1999; Olano et al. 2014; Schreiber et al. 2015; Lu et al. 2018), but at the cost of lower water conduction rates (Puchi et al. 2019). After the monsoon arrives, stimulated by a significant increase in precipitation, the cambium becomes active again, and the lumen diameter first increases slightly and then decreases again in latewood, eventually leading to fluctuations in wood density (Abe et al. 2003;

Vieira et al. 2010). This is consistent with the IADFs formation of Chinese pine in the Helan Mountains, as revealed by cambium activity monitoring (Gao et al. 2021b).

Tree-ring width synthesizes the complex signals of long-time scales in the previous year and the current year, while IADFs only respond to climatic events at a seasonal scale. The two are driven by different time-scale climatic conditions and record significantly different climatic signals. This conclusion is supported by other studies. For example, Olano et al. (2015) compared the response of *Juniperus thurifera* L. ring width and IADFs to climate in semi-humid and semi-arid regions of Spain, and found little overlapping climate signals between them. Pacheco et al. (2016) found that the growth of *Juniperus thurifera* L. and *Pinus halepensis* Mill. in the Mediterranean region was supported by humid and cold conditions from late winter to early spring, while the formation of L-IADFs was due to the wet conditions from late summer to early autumn and the heavy rainfall in midsummer.

Emergence of IADFs associated with the rainy season

Soil moisture fluctuations affect the generation and differentiation of xylem cells, thereby affecting the anatomical characteristics of tree rings (Vaganov et al. 2006). After a slow depletion and strong evaporation from early spring to summer, soil moisture in the study area reaches its lowest value of the year before the onset of the rainy season. Subsequently, the soil moisture content increases considerably due to monsoonal precipitation and remains high for a considerable period of time, its intra-annual dynamics showing a low–high-low trend similar to precipitation. However, when the rainy season is abnormally delayed, the severe deficit period of soil moisture in early summer will be prolonged. At this time, the number of cambium cells and enlarged cells reached their maximum, but the aggravation of drought forced the cambium activity to slow down and limited the cell enlargement, resulting in the emergence of IADFs (Rossi et al. 2009). Thus, the later the rainy season starts, the more IADFs appears (Fig. 6, Fig. 7). Similar relationships can be found in findings from other monsoon regions in Asia and North America. For example, Singh et al. (2016) attributed the formation of E-IADFs in *Pinus kesiya* in northeast India to dry conditions in the early growing season caused by insufficient monsoon rainfall. Babst et al. (2016) suggested that seasonal moisture limitation caused by the weak North American monsoon and favorable external conditions at the end of the growing season were important reasons for the emergence of E-IADFs at the end of earlywood of *Pinus ponderosa* in southern Arizona.

Drought in early summer causes IADFs while also promoting the transformation of earlywood to latewood (Arzac et al. 2018; Putz et al. 2021). The intermittent thunderstorms in the rainy season cause strong fluctuations in soil moisture, stimulate the reactivation of the cambium and increase the proportion of latewood (Camarero et al. 2010). This is why the IADFs in this study resemble the E + type formed in the transition zone between earlywood and latewood (E-IADFs were subdivided into E and E + based on their different positions in earlywood) (De Micco et al. 2016), and the IADFs frequency is significantly positively correlated with LW_{adj}. It should be pointed out here that our IADFs are generated in the middle and late growing seasons, which is different from the IADFs that appear in the early growing season, but they are all abnormal structures that occur in sectors that are supposed to grow earlywood, so we tend to classify them as E-type. Our conclusion is consistent with previous studies (De Micco et al. 2016; Zhang et al. 2020; Gao et al. 2021b), that the negative effects of summer drought on tree growth are reversible and can be partially compensated by short-term growth recovery triggered by rainfall events.

Conclusion

The growth of Chinese pine in the eastern margin of the CLP correlated with the soil moisture at the end of the growing season of the previous year and in the spring of the current year, whereas IADFs responded only to intra-annual climatic events, and they record distinct climatic signals. The formation of IADFs in Chinese pine is coupled with drought stress during early summer, which may be related to the late start of the rainy season. Suitable conditions after water deficit resulted in anomalous changes in latewood density, making the E-IADFs look more like E +, and the frequency of IADFs was significantly positively correlated with LW_{adj}. This reflects the trade-off between xylem hydraulic security and water transport rate for trees to adapt to seasonal fluctuations in water, thus forming a bimodal growth pattern similar to trees in the Mediterranean climates. The seasonal growth dynamics of Chinese pine in the eastern edge of the CLP provide useful insights for regional climate change as well as the possibility of quantifying long-term monsoon variability.

Supplementary Information The online version contains supplementary material available at https://doi.org/10.1007/s00484-023-02459-7.

Acknowledgements The author would like to thank the editors, Dr. Hung Nguyen, and another anonymous reviewer for their valuable comments.

Funding This work was supported by the National Natural Science Foundation of China (Grant No. 41790421 and 42071057).

Data Availability Data that have contributed to the reported results are available from the corresponding author on request.

Declarations

Conflict of interest The authors declare no competing interests.

References

Abe H, Nakai T (1999) Effect of the water status within a tree on tracheid morphogenesis in *Cryptomeria japonica* D. Don Trees 14:124–129

Abe H, Nakai T, Utsumi Y, Kagawa A (2003) Temporal water deficit and wood formation in *Cryptomeria japonica*. Tree Physiol 23:859–863

Arzac A, Rozas V, Rozenberg P, Olano JM (2018) Water availability controls *Pinus pinaster* xylem growth and density: a multiproxy approach along its environmental range. Agric for Meteorol 250:171–180

Babst F, Wright WE, Szejner P, Wells L, Belmecheri S, Monson RK (2016) Blue intensity parameters derived from Ponderosa pine tree rings characterize intra-annual density fluctuations and reveal seasonally divergent water limitations. Trees 30:1403–1415

Battipaglia G, Campelo F, Vieira J, Grabner M, De Micco V, Nabais C, Cherubini P, Carrer M, Bräuning A, Čufar K (2016) Structure and function of intra–annual density fluctuations: mind the gaps. Front Plant Sci 7:595

Beguería S, Vicente-Serrano SM, Beguería MS (2017) SPEI: calculation of the standardised precipitation-evapotranspiration index. Available at:https://CRAN.R-project.org/package=SPEI (Accessed September 10, 2022)

Begum S, Nakaba S, Yamagishi Y, Oribe Y, Funada R (2013) Regulation of cambial activity in relation to environmental conditions: understanding the role of temperature in wood formation of trees. Physiol Plant 147:46–54

Bo M, Guo Y, Tao H, Liu G, Li S, Pu W (2015) SPEIPM-based research on drought impact on maize yield in North China Plain. J Integr Agric 14:660–669

Camarero JJ, Olano JM, Parras A (2010) Plastic bimodal xylogenesis in conifers from continental Mediterranean climates. New Phytol 185:471–480

Campelo F, Nabais C, Freitas H, Gutiérrez E (2007) Climatic significance of tree-ring width and intra-annual density fluctuations in *Pinus pinea* from a dry Mediterranean area in Portugal. Ann for Sci 64:229–238

Chen F, Yuan Y, Zhang R, Qin L (2014) A tree-ring based drought reconstruction (AD 1760–2010) for the Loess Plateau and its possible driving mechanisms. Global Planet Change 122:82–88

Cook ER (1985) A time series analysis approach to tree ring standardization. Univ Arizona Tucson p 89–105

Cuny HE, Rathgeber CBK, Frank D, Fonti P, Fournier M (2014) Kinetics of tracheid development explain conifer tree-ring structure. New Phytol 203:1231–1241

Dai X, Wang P, Chou J (2003) Multiscale characteristics of the rainy season rainfall and interdecadal decaying of summer monsoon in North China. Chin Sci Bull 48:2730–2734

De Luis M, Novak K, Raventos J, Gricar J, Prislan P, Cufar K (2011) Cambial activity, wood formation and sapling survival of *Pinus halepensis* exposed to different irrigation regimes. For Ecol Manage 262:1630–1638

De Micco V, Campelo F, De Luis M, Bräuning A, Grabner M, Battipaglia G, Cherubini P (2016) Intra-annual density fluctuations in tree rings: how, when, where, and why? IAWA J 37:232–259

Ding Y, Wang Z, Sun Y (2008) Inter-decadal variation of the summer precipitation in East China and its association with decreasing Asian summer monsoon. Part I: Observed evidences. Int J Climatol 28:1139–1161

Eilmann B, Zweifel R, Buchmann N, Fonti P, Rigling A (2009) Drought-induced adaptation of the xylem in Scots pine and pubescent oak. Tree Physiol 29:1011–1020

Eilmann B, Zweifel R, Buchmann N, Pannatier EG, Rigling A (2011) Drought alters timing, quantity, and quality of wood formation in Scots pine. J Exp Bot 62:2763–2771

Fang K, Gou X, Chen F, Liu C, Davi N, Li J, Zhao Z, Li Y (2012) Tree-ring based reconstruction of drought variability (1615–2009) in the Kongtong Mountain area, northern China. Global Planet Change 80:190–197

Fonti P, von Arx G, García-González I, Eilmann B, Sass-Klaassen U, Gärtner H, Eckstein D (2010) Studying global change through investigation of the plastic responses of xylem anatomy in tree rings. New Phytol 185:42–53

Gao J, Rossi S, Yang B (2021a) Origin of intra-annual density fluctuations in a semi-arid area of northwestern China. Front Plant Sci 12:777753

Gao J, Yang B, Peng X, Rossi S (2021b) Tracheid development under a drought event producing intra-annual density fluctuations in the semi-arid China. Agric For Meteorol 308:108572

Gruber A, Strobl S, Veit B, Oberhuber W (2010) Impact of drought on the temporal dynamics of wood formation in *Pinus sylvestris*. Tree Physiol 30:490–501

Holmes RL (1983) Computer-assisted quality control in tree-ring dating and measurement. Tree-Ring Bull 43:51–67

Hsiao TC (1973) Plant responses to water stress. Annu Rev Plant Physiol 24:519–570

Kagawa A, Sugimoto A, Maximov TC (2006) 13CO2 pulse-labelling of photoassimilates reveals carbon allocation within and between tree rings. Plant, Cell Environ 29:1571–1584

Larsen CPS, MacDonald GM (1995) Relations between tree-ring widths, climate, and annual area burned in the boreal forest of Alberta. Can J for Res 25:1746–1755

Li Y (2013) Characteristic analysis of summer unimodal and bimodal precipitation process in North China. Nanjing Univ Inf Sci Technol p 19–27. (in Chinese)

Li Y, Guo P (2015) Characteristics and mechanisms of unimodal and bimodal precipitation processes in North China in summer. Trans Atmos Sci 38:540–548 (in Chinese)

Li Q, Deng Y, Wang S, Gao L, Gou X (2022) A half-millennium perspective on recent drying in the eastern Chinese Loess Plateau. CATENA 212:106087

Lockhart JA (1965) An analysis of irreversible plant cell elongation. J Theor Biol 8:264–275

Lu W, Yu X, Jia G, Li H, Liu Z (2018) Responses of intrinsic water-use efficiency and tree growth to climate change in semi-arid areas of North China. Sci Rep 8:1–10

Ma Z, Dan L (2005) Dry/wet variation and its relationship with regional warming in arid-regions of Northern China. Chin J Geophys 48:1091–1099

Ma Z, Fu C (2006) Some evidence of drying trend over northern China from 1951 to 2004. Chin Sci Bull 51:2913–2925

Martin-Benito D, Beeckman H, Canellas I (2013) Influence of drought on tree rings and tracheid features of *Pinus nigra* and *Pinus sylvestris* in a mesic Mediterranean forest. Eur J Forest Res 132:33–45

Meko DM, Baisan CH (2001) Pilot study of latewood-width of conifers as an indicator of variability of summer rainfall in the North American Monsoon Region. Int J Climatol 21:697–708

Nonami H, Boyer JS (1990) Primary events regulating stem growth at low water potentials. Plant Physiol 93:1601–1609

Novak K, Sánchez MAS, Čufar K, Raventós J, Luis MD (2013) Age, climate and intra-annual density fluctuations in *Pinus halepensis* in Spain. IAWA J 34:459–474

Olano JM, Linares JC, García-Cervigón AI, Arzac A, Delgado A, Rozas V (2014) Drought-induced increase in water-use efficiency reduces secondary tree growth and tracheid wall thickness in a Mediterranean conifer. Oecologia 176:273–283

Olano JM, Garcia-Cervigon AI, Arzac A, Rozas V (2015) Intra-annual wood density fluctuations and tree-ring width patterns are sex- and site-dependent in the dioecious conifer *Juniperus thurifera* L. Trees-Struct Funct 29:1341–1353

Pacheco A, Camarero JJ, Carrer M (2016) Linking wood anatomy and xylogenesis allows pinpointing of climate and drought influences on growth of coexisting conifers in continental Mediterranean climate. Tree Physiol 36:502–512

Pacheco A, Camarero JJ, Pompa-García M, Battipaglia G, Voltas J, Carrer M (2020) Growth, wood anatomy and stable isotopes show species-specific couplings in three Mexican conifers inhabiting drought-prone areas. Sci Total Environ 698:134055

Panayotov MP, Zafirov N, Cherubini P (2013) Fingerprints of extreme climate events in *Pinus sylvestris* tree rings from Bulgaria. Trees-Struct Funct 27:211–227

Peters RL, Steppe K, Cuny HE, De Pauw DJW, Frank DC, Schaub M, Rathgeber CBK, Cabon A, Fonti P (2021) Turgor – a limiting factor for radial growth in mature conifers along an elevational gradient. New Phytol 229:213–229

Piermattei A, Campelo F, Buntgen U, Crivellaro A, Garbarino M, Urbinati C (2020) Intra-annual density fluctuations (IADFs) in *Pinus nigr*a (J. F. Arnold) at high-elevation in the central Apennines (Italy). Trees-Struct Funct 34:771–781

Puchi PF, Castagneri D, Rossi S, Carrer M (2019) Wood anatomical traits in black spruce reveal latent water constraints on the boreal forest. Glob Change Biol 26:1767–1777

Putz TR, Urza AK, Hankin LE, Bisbing SM (2021) Seasonal water availability drives trait variation in isolated basin and range *Pinus ponderosa*. For Ecol Manage 488:119022

Qin Z, Tang H, Li W, Zhang H, Zhao S, Wang Q (2014) Modelling impact of agro-drought on grain production in China. Int J Disaster Risk Reduction 7:109–121

Rao MP, Cook ER, Cook BI, Anchukaitis KJ, D'Arrigo RD, Krusic PJ, LeGrande AN (2019) A double bootstrap approach to Superposed Epoch Analysis to evaluate response uncertainty. Dendrochronologia 55:119–124

Rolland C (1993) Tree-ring and climate relationships for *Abies alba* in the internal Alps. Tree-Ring Bull 53:1–11

Rossi S, Simard S, Rathgeber CBK, Deslauriers A, De Zan C (2009) Effects of a 20-day-long dry period on cambial and apical meristem growth in *Abies balsamea* seedlings. Trees 23:85–93

Schreiber SG, Hacke UG, Hamann A (2015) Variation of xylem vessel diameters across a climate gradient: insight from a reciprocal transplant experiment with a widespread boreal tree. Funct Ecol 29:1392–1401

Singh ND, Yadav RR, Venugopal N, Singh V, Yadava AK, Misra KG, Singh TB, Sanjita C (2016) Climate control on ring width and intra-annual density fluctuations in *Pinus kesiya* growing in a sub-tropical forest of Manipur, Northeast India. Trees 30:1711–1721

Song H, Liu Y (2011) PDSI variations at Kongtong Mountain, China, inferred from a 283-year Pinus tabulaeformis ring width chronology. J Geophys Res-Atmos 116:D22111

Stokes MA, Smiley TL (1968) An introduction to tree-ring dating. University of Arizona Press p 11–18

Swidrak I, Gruber A, Oberhuber W (2011) Cambial activity and xylem cell development in *Pinus cembra* and *Pinus sylvestris* at their climatic limits in the eastern Alps in 2007. Phyton-Annales Rei Botanicae 51:299–313

Vaganov EA, Hughes MK, Shashkin AV (2006) Growth dynamics of conifer tree rings: images of past and future environments. Ecol Stud 183:281–306

Vicente-Serrano SM, Beguería S, López-Moreno JI (2010) A multiscalar drought index sensitive to global warming: the standardized precipitation evapotranspiration index. J Clim 23:1696–1718

Vieira J, Campelo F, Nabais C (2010) Intra-annual density fluctuations of P*inus pinaster* are a record of climatic changes in the western Mediterranean region. Can J for Res 40:1567–1575

Vieira J, Nabais C, Rossi S, Carvalho A, Freitas H, Campelo F (2017) Rain exclusion affects cambial activity in adult maritime pines. Agric for Meteorol 237:303–310

Wang H (2001) The weakening of the Asian monsoon circulation after the end of 1970's. Adv Atmos Sci 18:376–386

Wood SN (2006) Generalized additive models: an introduction with R. Chapman and Hall/CRC p496

Yu R, Wang B, Zhou T (2004) Tropospheric cooling and summer monsoon weakening trend over East Asia. Geophys Res Lett 31:L22212

Zalloni E, de Luis M, Campelo F, Novak K, De Micco V, Di Filippo A, Vieira J, Nabais C, Rozas V, Battipaglia G (2016) Climatic signals from intra-annual density fluctuation frequency in mediterranean pines at a regional scale. Front Plant Sci 7:00579

Zalloni E, Battipaglia G, Cherubini P, Saurer M, De Micco V (2019) Wood growth in pure and mixed *Quercus ilex* L. forests: drought influence depends on site conditions. Front Plant Sci 10:00397

Zhang L, Xiao J, Zhou Y, Zheng Y, Li J, Xiao H (2016) Drought events and their effects on vegetation productivity in China. Ecosphere 7:e01591

Zhang J, Alexander MR, Gou X, Deslauriers A, Fonti P, Zhang F, Pederson N (2020) Extended xylogenesis and stem biomass production in *Juniperus przewalskii* Kom. during extreme late-season climatic events. Ann for Sci 77:1–11

Zhao A, Zhang A, Liu J, Feng L, Zhao Y (2019) Assessing the effects of drought and "Grain for Green" program on vegetation dynamics in Chin's Loess Plateau from 2000 to 2014. CATENA 175:446–455

Zhu L, Li Z, Wang X (2017) Anatomical characteristics of xylem in tree rings and its relationship with environments. Chin J Plant Ecol 41:238–251 (in Chinese)